PHYSICAL REVIEW B **80**, 054512 (2009)

Pairing resonance as a normal-state spin probe in ultrathin Al films

G. Catelani
Department of Physics and Astronomy, Rutgers University, Piscataway, New Jersey 08854, USA

Y. M. Xiong, X. S. Wu,* and P. W. Adams
Department of Physics and Astronomy, Louisiana State University, Baton Rouge, Louisiana 70803, USA
(Received 5 May 2009; published 18 August 2009)

We present a quantitative analysis of the low-temperature, high parallel-field pairing resonance in ultrathin superconducting Al films with dimensionless conductance $g \gg 1$. In this regime we derive an analytical expression for the tunneling density-of-states spectrum from which a variety of normal-state spin parameters can be extracted. We show that by fitting tunneling data at several supercritical parallel magnetic fields we can determine all of the relevant parameters that have traditionally been obtained via fits to tunneling data in the superconducting phase. These include the spin-orbit scattering rate, the antisymmetric Landau parameter G^0, and the orbital pair-breaking parameter.

DOI: 10.1103/PhysRevB.80.054512 PACS number(s): 74.50.+r, 74.40.+k, 74.78.Db, 73.50.Fq

I. INTRODUCTION

Determining the microscopic spin parameters of paramagnetic metals has historically been a process fraught with complications and inaccuracies.[1,2] In general, the spin response of an interacting fermionic system can be modified by spin-orbit scattering processes, electron-phonon interactions, and/or electron-electron interactions.[3,4] These contributions to the spin susceptibility themselves can be affected by disorder,[5,6] dimensionality,[7,8] and the presence of interfaces.[9] The two primary spin parameters for a paramagnetic system are the spin-orbit scattering rate and the antisymmetric $l=0$ Landau parameter G^0. The latter accounts for the renormalization of the bare Pauli spin susceptibility due to electron-phonon and electron-electron interactions. Depending upon the sign of this parameter the effective spin moment can be larger or smaller than the bare electron value. In practice, the spin-orbit scattering rate can be obtained from the coherent backscattering contributions to the magnetoresistance of moderately disordered nonsuperconducting films or by parallel magnetic field studies of thin superconducting films. The Fermi-liquid parameter G^0, however, is more difficult to determine accurately. In principle, it can be extracted from low-temperature measurements of the spin susceptibility χ and the heat capacity γ from which the respective corresponding density of states $N(\chi)$ and $N(\gamma)$ are obtained. The ratio of these densities of states is a direct measure of the many-body renormalization, $G^0=N(\gamma)/N(\chi)-1$.[3] Unfortunately, orbital contributions to the susceptibility make it very difficult to determine its spin component precisely in high-conductivity systems and phonon contributions to the specific heat can introduce significant systematic errors in the measurement of $N(\gamma)$. In this report we address the determination of G^0 and the spin-orbit scattering rate via the Pauli-limited, normal-state pairing resonance.[10–13]

If a paramagnetic system has a superconducting phase and can be made into a thin-film form, then it is possible to access the spin parameters through tunneling density-of-states (DOS) measurements. A Zeeman splitting of the BCS coherence peaks can be induced by applying a parallel magnetic field to a film of thickness $t \ll \xi$, where ξ is the superconducting coherence length. Tedrow and Meservey pioneered the use of superconducting spin-resolved tunneling to directly measure both spin-orbit scattering rate and the Landau parameter G^0 in thin Al and Ga films near the parallel critical-field transition.[1,14,15] This technique, however, cannot access G^0 well into the superconducting phase since those electrons responsible for the exchange effects are consumed by the formation of the condensate.[16] To circumvent this limitation, one needs to measure the Zeeman splittings in magnetic fields just below parallel critical field. However, one cannot completely reach the normal-state quasiparticle density in a thin film while remaining in the superconducting phase since the spin-paramagnetically limited parallel critical-field transition is first order. Because of this, one must extrapolate the normal-state value of G^0 from data taken in the superconducting phase. Alternatively, the films can be made marginally thicker, which will suppress the first-order transition,[16] or the measurements can be made at higher temperatures. But these strategies limit one to a very narrow range of film thicknesses. Furthermore, in both cases one is constrained to a very narrow range of applied fields.

Here we present a detailed analysis of the normal-state pairing resonance (PR) from which the spin-orbit scattering rate, orbital depairing parameter, and the Landau parameter G^0 can be accurately obtained. We show that the technique can be used over a wide range of film thicknesses and resistances. Moreover, the measurements can be made in fields well above the parallel critical field and in fields substantially tilted away from parallel orientation.[17,18]

II. PAIRING RESONANCE IN PARALLEL FIELD

The PR is characterized, as any other resonance, by two quantities: its position and its width. The former is given by[11]

$$E_+ = \frac{1}{2}(E_Z + \Omega), \tag{1}$$

where

$$E_Z = \frac{2\mu_B H}{1+G^0} \tag{2}$$

is the Zeeman energy renormalized by the Fermi-liquid parameter G^0, μ_B is the Bohr magneton, and

$$\Omega = \sqrt{E_Z^2 - \Delta_0^2} \tag{3}$$

is the Cooper-pair energy with Δ_0 the zero-field, zero-temperature gap of the corresponding superconducting phase.

The width of the PR depends on the effective dimensionality of the sample and on the strength Γ of pair-breaking mechanisms other than the Zeeman splitting. If these are absent, a nonperturbative approach is necessary (see Ref. 11), and for quasi-two-dimensional systems the width is

$$W_2 = \frac{\Delta_0^2}{4g\Omega}, \tag{4}$$

where $g=4\pi\hbar\nu_0 D$ is the dimensionless conductance with D the diffusion constant and ν_0 the bare DOS. If $W_2 \ll \Gamma$ then a perturbative calculation is sufficient to accurately estimate the width, provided one properly takes into account the role of the exclusion principle.[18] For instance, in the case of a tilted magnetic field, Γ is proportional to the perpendicular component of the field and the exclusion principle both shifts and reshapes the PR. If we consider the effects of spin-orbit scattering and the finite-thickness orbital contributions of the parallel field,[19] then

$$\frac{\Gamma}{2\Delta_0} = b + c\left(\frac{\mu_B H}{\Delta_0}\right)^2, \tag{5}$$

where according to the notation commonly used to characterize the DOS in the superconducting state,[20]

$$b = \frac{\hbar}{3\tau_{so}\Delta_0} \tag{6}$$

is proportional to the spin-orbit scattering rate $1/\tau_{so}$ and

$$c = \frac{De^2t^3\Delta_0}{8\ell\mu_B^2\hbar} \tag{7}$$

is the orbital depairing parameter, where t is the film's thickness, e is the electron charge, and ℓ is the mean-free path. This latter parameter quantifies the strength of the orbital effect of the field[21] in relation to the Zeeman effect. The Zeeman splitting is the dominant pair-breaking mechanism for $c \lesssim 1$.

Following the procedure outlined in Ref. 18, we obtain the zero-temperature correction to the (spin-down) DOS due to the PR

$$\frac{\delta\nu(\epsilon)}{\nu_0} = -A(\epsilon;E_Z,\Gamma)\frac{W_2\Gamma}{(\epsilon-E_+)^2+\Gamma^2}, \tag{8}$$

where ϵ is the energy measured from the Fermi level; the other quantities entering this formula have been defined above, see Eqs. (1)–(5). The correction for the other spin component is found by replacing $\epsilon \to -\epsilon$ in the right-hand side of Eq. (8). The function

$$A(\epsilon;E_Z,\Gamma) = \frac{1}{\pi}\{\arctan[(E_Z-\epsilon)/\Gamma] + \arctan[\Omega/\Gamma] + \arctan[(\epsilon-\Omega)/\Gamma] + \arctan[(2\epsilon-E_Z)/\Gamma]\} \tag{9}$$

accounts for the exclusion principle and takes on values between 0 and 2. It alters the Lorentzian shape of the PR, especially at energies close to the Fermi energy (i.e., $\epsilon \ll E_+$) and, in fact, $A(\epsilon=0)=0$. We note that Eqs. (8) and (9) imply that $\delta\nu/\nu_0 \leq 2W_2/\Gamma$, which is consistent with the assumed perturbative criterion $\Gamma \gg W_2$.

In this work we show that Eq. (8) gives a quantitative description of the PR and that it enables us to extract from normal-state measurements the physical quantities G^0, b, and c. While they can be obtained from DOS measurements in the superconducting state,[15,16] this requires to solve a set of self-consistent equations for the order parameter and "molecular" magnetic field together with the Usadel equations for the normal and anomalous Green's functions—a much more complicated task in comparison to the simple fitting of the data that we describe in Sec. IV.

III. EXPERIMENTAL PROCEDURE

Aluminum films were grown by e-beam deposition of 99.999% Al stock onto fire-polished glass-microscope slides held at 84 K. The depositions were made at a rate of $\sim$0.1 nm/s in a typical vacuum $P < 3\times10^{-7}$ Torr. A series of films with thicknesses ranging from 2 to 2.9 nm had a dimensionless normal-state conductance that ranged from $g=5.6$ to 230 at 100 mK. After deposition, the films were exposed to the atmosphere for 10–30 min in order to allow a thin native oxide layer to form. Then a 9-nm-thick Al counterelectrode was deposited onto the film with the oxide serving as the tunneling barrier. The counterelectrode had a parallel critical field of $\sim$2.7 T due to its relatively large thickness, which is to be compared with $H_{c\|}\sim 6$ T for the films. The junction area was about 1 mm$\times$1 mm, while the junction resistance ranged from 10–100 kΩ, depending on exposure time and other factors. Only junctions with resistances much greater than that of the films were used. Measurements of resistance and tunneling were carried out on an Oxford dilution refrigerator using a standard ac four-probe technique. Magnetic fields of up to 9 T were applied using a superconducting solenoid. A mechanical rotator was employed to orient the sample *in situ* with a precision of $\sim 0.1°$.

IV. RESULTS AND DISCUSSION

We show in Fig. 1 the tunneling conductance measured at 70 mK and three supercritical parallel magnetic fields. This particular film of dimensionless conductance $g \simeq 57$ was 2.6 nm thick and had a zero-field superconducting transition temperature $T_c=2.74$ K. Common to the three data sets is the Coulomb zero-bias anomaly (ZBA),[22] which produces a logarithmic depletion in the DOS at high biases; the logarithm is cutoff at low bias by temperature. In order to isolate the paramagnetic resonance, we need to remove the contri-

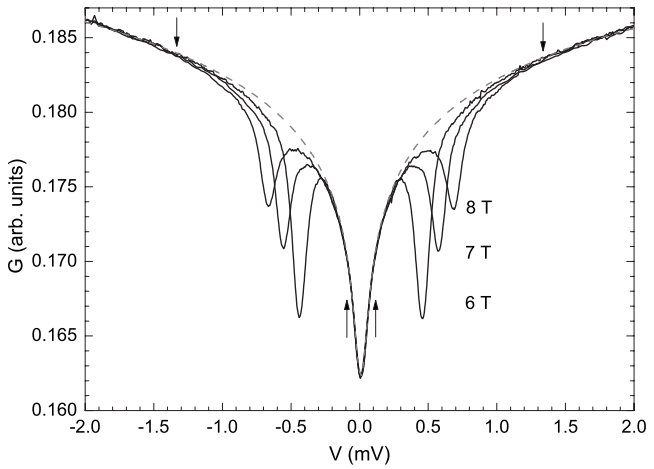

FIG. 1. Tunneling conductance at 70 mK for three supercritical parallel magnetic fields (solid lines). The dashed line is the best fit to the zero-bias anomaly due to Coulomb interaction. The arrows point to the boundaries of the low- ($|V| \lesssim 0.2$ mV) and high-bias ($|V| \gtrsim 1.4$ mV) regions used for the fitting.

bution of the ZBA. To interpolate between the low- and high-bias parts of the curves (as delimited by the arrows in Fig. 1), we find the best-fit curve, restricted to these regions, given by the sum of a background constant tunneling conductance and Re $\Psi(1/2+i\alpha V)$, where Ψ is the digamma function and α a fitting parameter. The result is the dashed curve in Fig. 1, which is then subtracted from the measured tunneling conductances.

In Fig. 2 we plot with a solid line the PR at 7 T obtained as described above. As discussed in Sec. II, its position and width are, respectively, determined by the Zeeman energy E_Z and the pair-braking rate Γ while the conductance g only affects the overall magnitude. Using Eq. (8), the best fit to the data is given by the dot-dashed curve; while the main peak is well reproduced, a shoulder feature at higher bias is underestimated. To our knowledge, there are two possible

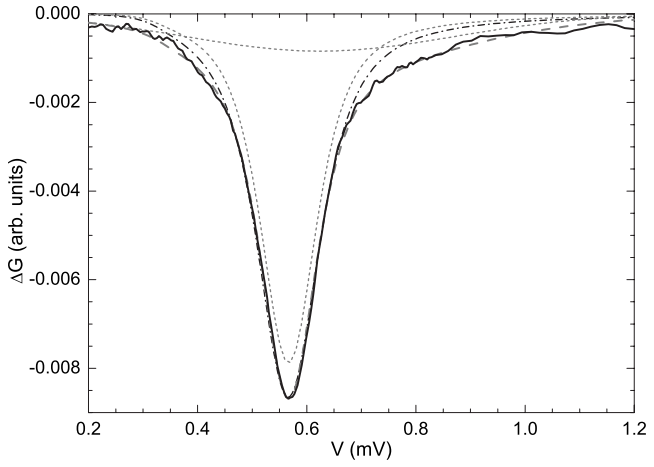

FIG. 2. Pairing resonance at 7 T (solid line) with the ZBA subtracted off. The dot-dashed curve is the best fit to the data using Eq. (8). The dashed curve is the best fit with a sum of Eq. (8) and a Gaussian—see the text for more details on the fitting procedure. The two terms of the sum are plotted separately as dotted curves.

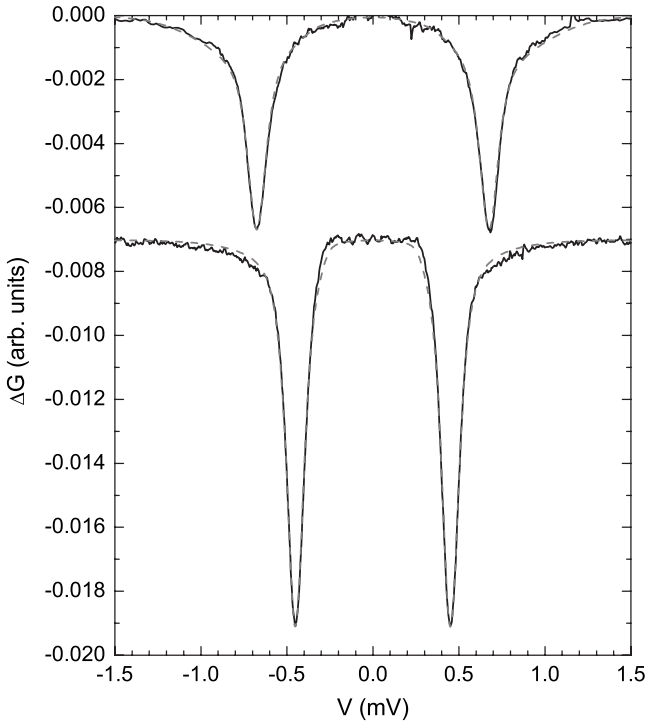

FIG. 3. Pairing resonances measured at 8 T (top) and 6 T (bottom solid curve). The bottom curve is shifted down by 0.007 for clarity. The dashed lines are best fits to the data obtained as described in the text. The asymmetry of the PR and its suppression near the Fermi energy are easily recognized in the data taken at 6 T.

causes for this discrepancy, namely, a finite bias, triplet channel anomaly,[22] similar to the Coulomb ZBA but much weaker, and finite-temperature effects.[23] To take into account these possible corrections, we add to Eq. (8) a Gaussian contribution; to reduce the number of free parameters, we require it to be centered at the Zeeman energy, which is where a triplet channel correction would be located, while the amplitude and width are used as fitting parameters. The best fit thus found is the dashed line in Fig. 2; the peaked PR and broad Gaussian contributions are plotted separately with dotted lines.

We present in Fig. 3 two more PRs with the best-fit curves. The asymmetric shape of the resonance and its suppression near the Fermi energy are evident in the lowest-field data. We note that fitting these data with Eq. (8) only would require us to decrease the conductance with increasing field, whereas we can use the same value of the conductance at all fields when the Gaussian correction is included. Moreover, the value of the Zeeman energy is only weakly affected by the inclusion of this correction, with the change in E_Z smaller than our estimated relative error of about 1%. While these two observations support the validity of our approach, the magnitude of the width parameter Γ turns out to be more sensitive to the Gaussian correction. However, its field dependence (see Fig. 5) is robust and the quantitative estimates discussed below are in line with expectations.

Having detailed our fitting procedure, we now consider the physical quantities that can be extracted from the data. In Fig. 4 we plot the normalized Zeeman energy as a function

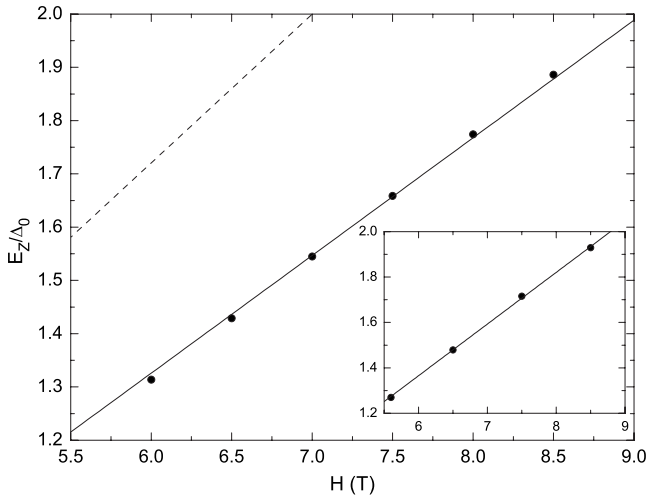

FIG. 4. Normalized Zeeman energy E_Z/Δ_0 vs magnetic field H. The solid line is the best fit to Eq. (2); the slope is proportional to $(1+G^0)^{-1}$ and we estimate the value of the Fermi-liquid parameter $G^0 \simeq 0.26$. For comparison, the dashed line represents the expected linear relationship in the absence of Fermi-liquid renormalization. Inset: same plot as the main figure but for a thicker film with $G^0 \simeq 0.24$ (see text for details).

of the applied field. By fitting the data with Eq. (2) we find $G^0 \simeq 0.26$; a similar estimate, $G^0 \simeq 0.24$, is obtained for a thicker film with $t=2.9$ nm, $g=230$, and zero-field, zero-temperature gap $\Delta_0=0.41$ meV, see the inset of Fig. 4. We note that a better fit to the data in Fig. 4 could be obtained by allowing for a finite negative intercept; however, the large estimated error on the intercept makes the best-fit line compatible with the expectation that it passes through the origin [see Eq. (2)]. This finite intercept could be due to small higher-order contributions since at the lowest field the parameter $2W_2/\Gamma \simeq 0.07$ is only marginally smaller than 1. In support to this interpretation, we find no evidence of finite intercept for the thicker film for which $2W_2/\Gamma \lesssim 0.016$. Alternatively, the intercept could be an additional indication, together with the shoulder feature mentioned above, of finite-temperature effects. We will further investigate this latter issue in a separate work.

The width parameter Γ is plotted in Fig. 5 as a function of $(\mu_B H/\Delta_0)^2$ together with the best-fit line. According to Eq. (5), the intercept and the slope are determined by the spin-orbit parameter b and orbital parameter c, respectively. We estimate their values as $b \simeq 0.06$, in agreement with the results in the literature, and $c \simeq 0.02$, which favorably compares[24] with the value $c \simeq 0.04$ extrapolated from superconducting-state measurements in marginally thick (i.e., $c \simeq 1$) films. Repeating the analysis for the thicker film—see the inset of Fig. 5—we find $b \simeq 0.06$ and $c \simeq 0.04$. As a further check on the validity of the present approach, for this film we show in Fig. 6 the measured and calculated DOS in the normal and superconducting states for fields of 5.6 and 4 T, respectively: all the main features of the superconducting DOS are captured by the theoretical curve[25] obtained by solving the Usadel and self-consistent equations[15] with the parameters found via the normal-state measurements.

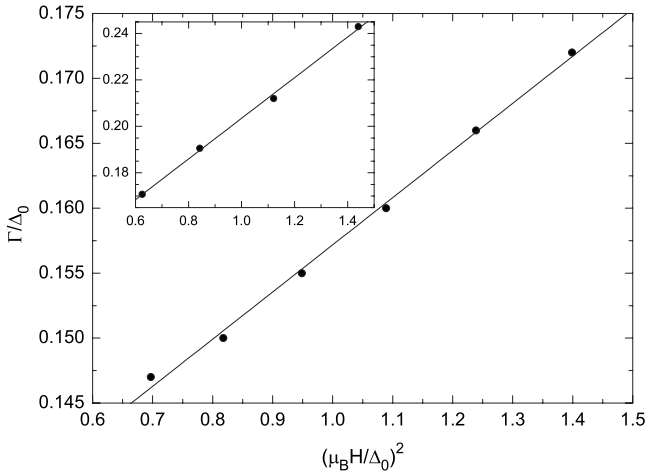

FIG. 5. Normalized pair-breaking parameter Γ/Δ_0 vs the square of the reduced field. Using the linear relationship in Eq. (5) we obtain from the best-fit line the spin-orbit scattering rate $b \simeq 0.06$ and the orbital effect parameter $c \simeq 0.02$. As in Fig. 4, we show in the inset the data pertaining to the 2.9-nm-thick film.

In summary, we have presented a quantitative study of the paramagnetic pairing resonance in parallel field. We have derived an expression, Eq. (8), for the density of states which takes into account spin-orbit scattering, orbital effect of the magnetic field, and the Pauli exclusion principle. The latter is responsible for the suppression of the resonance near the Fermi energy, see Fig. 3 and the left panel of Fig. 6. By fitting the PRs measured at different fields we have obtained the values of the Fermi-liquid parameter G^0, the spin-orbit scattering rate b, and the orbital parameter c, thus showing that normal-state experiments can provide the same information usually extracted from the DOS of the superconducting phase. Since the PR affects the spin-resolved DOS at opposite biases, it can, in fact, be used to probe the electron-spin polarization in magnetic films. The present work provides the foundation for the analysis of tunneling studies of itinerant magnetic systems via the PR.[26]

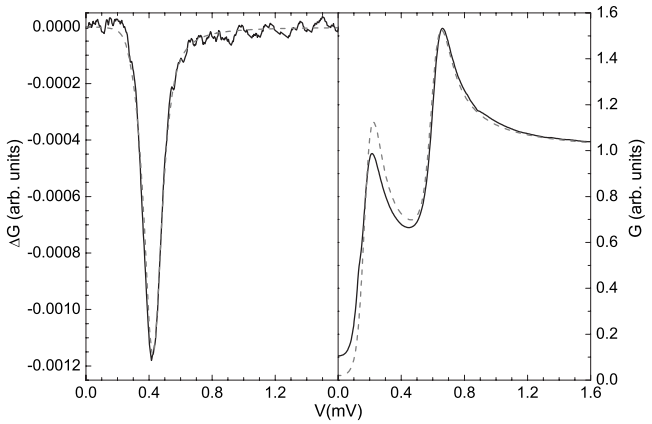

FIG. 6. Tunneling DOS in the normal (left, $H=5.6$ T) and superconducting (right, $H=4$ T) states at $T=70$ mK for a 2.9-nm-thick film. Solid lines are experimental data; dashed lines have been calculated with the parameters given in the text.

ACKNOWLEDGMENTS

We gratefully acknowledge enlightening discussions with Ilya Vekhter and Dan Sheehy. This work was supported by the DOE under Grant No. DE-FG02-07ER46420 for the experimental portion and by NSF under Grant No. NSF-DMR-0547769 (G.C.).

*Present address: School of Physics, Georgia Institute of Technology, Atlanta, Georgia 30332, USA.

[1] G. A. Gibson, P. M. Tedrow, and R. Meservey, Phys. Rev. B **40**, 137 (1989).
[2] D. C. Vier, D. W. Tolleth, and S. Schultz, Phys. Rev. B **29**, 88 (1984).
[3] G. Baym and C. Pethick, *Landau Fermi-Liquid Theory: Concepts and Applications* (John Wiley & Sons, New York, 1991).
[4] A. J. Leggett, Phys. Rev. **140**, A1869 (1965).
[5] B. L. Altshuler, A. G. Aronov, M. E. Gershenson, and Yu. V. Sharvin, Sov. Sci. Rev., Sect. A **9**, 223 (1987).
[6] G. Bergmann and C. Horriar-Esser, Phys. Rev. B **31**, 1161 (1985).
[7] A. P. Mackenzie and Y. Maeno, Rev. Mod. Phys. **75**, 657 (2003).
[8] I. L. Aleiner, D. E. Kharzeev, and A. M. Tsvelik, Phys. Rev. B **76**, 195415 (2007).
[9] L. P. Gor'kov and E. I. Rashba, Phys. Rev. Lett. **87**, 037004 (2001).
[10] W. Wu, J. Williams, and P. W. Adams, Phys. Rev. Lett. **77**, 1139 (1996).
[11] I. L. Aleiner and B. L. Altshuler, Phys. Rev. Lett. **79**, 4242 (1997); H. Y. Kee, I. L. Aleiner, and B. L. Altshuler, Phys. Rev. B **58**, 5757 (1998).
[12] V. Y. Butko, P. W. Adams, and I. L. Aleiner, Phys. Rev. Lett. **82**, 4284 (1999).
[13] P. W. Adams and V. Y. Butko, Physica B **284-288**, 673 (2000).
[14] P. M. Tedrow, J. T. Kucera, D. Rainer, and T. P. Orlando, Phys. Rev. Lett. **52**, 1637 (1984).
[15] J. A. X. Alexander, T. P. Orlando, D. Rainer, and P. M. Tedrow, Phys. Rev. B **31**, 5811 (1985).
[16] G. Catelani, X. S. Wu, and P. W. Adams, Phys. Rev. B **78**, 104515 (2008).
[17] X. S. Wu, P. W. Adams, and G. Catelani, Phys. Rev. Lett. **95**, 167001 (2005).
[18] G. Catelani, Phys. Rev. B **73**, 020503(R) (2006).
[19] In principle, inelastic-scattering effects should also be included. However, their contribution to the width Γ can be neglected; this point is discussed in some detail in Ref. 11.
[20] P. Fulde, Adv. Phys. **22**, 667 (1973).
[21] This definition is applicable in the limit $t \ll \ell$ of interest here.
[22] B. L. Altshuler and A. G. Aronov, in *Electron-Electron Interaction in Disordered Systems*, edited by A. L. Efros and M. Pollak (North-Holland, Amsterdam, 1985).
[23] We note that the small finite-temperature broadening due to the usual convolution with the derivative of the Fermi-Dirac distribution function has been taken into account.
[24] The actual film thickness is less than the nominal one due to the oxidation (see Sec. III) and extrapolation from thicker films overestimates c.
[25] In calculating the superconducting DOS we have introduced a small broadening of the same order of magnitude used in Ref. 16.
[26] Y. M. Xiong, P. W. Adams, and G. Catelani, Phys. Rev. Lett. **103**, 067009 (2009).